Slower Evolution of Human Immunodeficiency Virus Type 1 Quasispecies during Progression to AIDS

ERIC L. DELWART,[1]* HENG PAN,[1] HAYNES W. SHEPPARD,[2] DAVID WOLPERT,[3]
AVIDAN U. NEUMANN,[3,4] BETTE KORBER,[3] AND JAMES I. MULLINS[5]

*Aaron Diamond AIDS Research Center, The Rockefeller University, New York, New York 10016[1];
Viral and Rickettsial Disease Laboratory, California Department of Health Services, Berkeley, California 90704[2];
Santa Fe Institute, Santa Fe, New Mexico 87501[3]; Theoretical Biology and Biophysics, Los Alamos National
Laboratory, Los Alamos, New Mexico 87454[4]; and Department of Microbiology and Medicine,
University of Washington, Seattle, Washington 98195[5]*

The evolution of human immunodeficiency virus type 1 (HIV-1) quasispecies at the envelope gene was studied from the time of infection in 11 men who experienced different rates of CD4+ cell count decline and 6 men with unknown dates of infection by using DNA heteroduplex mobility assays. Quasispecies were genetically homogeneous near the time of seroconversion. Subsequently, slower proviral genetic diversification and higher plasma viremia correlated with rapid CD4+ cell count decline. Except for the fastest progressors to AIDS, highly diverse quasispecies developed in all subjects within 3 to 4 years. High quasispecies diversity was then maintained for years until again becoming more homogeneous in a subset of late-stage AIDS patients. Individuals who maintained high CD4+ cell counts showed continuous genetic turnover of their complex proviral quasispecies, while more closely related sets of variants were found in longitudinal samples of severely immunocompromised patients. The limited number of variants that grew out in short-term PBMC cocultures were rare in the uncultured proviral quasispecies of healthy, long-term infected individuals but more common in vivo in patients with low CD4+ cell counts. The slower evolution of HIV-1 observed during rapid progression to AIDS and in advanced patients may reflect ineffective host-mediated selection pressures on replicating quasispecies.

The high level of human immunodeficiency virus type 1 (HIV-1) genetic diversity seen within some infected individuals is the result of rapid and mutation-prone replication of large viral populations (9, 23, 46, 63, 66, 70, 83, 84). The resulting HIV-1 genetic diversity presumably accounts for viral population resilience despite ongoing immune responses and initially effective antiviral drug monotherapies (4, 9).

Following primary infection with HIV-1, some individuals develop AIDS within months (47, 59, 79) while others remain healthy with elevated CD4+ cell counts more than 15 years postinfection (7, 64, 75). Long-term infected asymptomatic subjects typically harbor lower plasma viral (7, 24, 28, 52, 62, 66) and peripheral blood mononuclear cell (PBMC) proviral burdens (7, 10, 41, 77) and develop stronger anti-p24 antibody responses (20, 24, 30, 72, 74, 80, 93), neutralizing antibody titers (7, 54, 62), and anti-HIV-1 cytotoxic T-lymphocyte responses (32, 68, 69) than do more-typical progressors to AIDS. Extremely rapid progressors to AIDS may develop only very weak humoral immune responses to HIV-1 (33, 47, 50, 59). Whether differences in viral loads, immune responses, and disease progression rate are generally due to viral (11) or host (12, 25, 29) factors or the precise combination of both remains unclear.

A wealth of information attests to the highly adaptable nature of HIV-1 quasispecies replicating in vivo. Mutant viruses with reduced susceptibility to antiviral drugs, detected within weeks of onset of monotherapy, represent the clearest examples of positive selection (43, 67, 84). Studies of HIV-1 and simian immunodeficiency virus evolution in vivo have reported a high ratio of nonsynonymous to synonymous site mutations (dN/dS ratio), likely reflecting selection for phenotypic changes (6, 60, 76, 78). Higher dN/dS ratios have been associated with slow progression to AIDS in both adults and children (3, 21, 44, 45, 89). The selective forces driving such evolution may include strong and changing immune responses (1, 2, 4, 5, 36, 48, 65, 89) as well as viral adaptation to growth in different cell types (8, 19, 26, 33, 35). The emergence of viruses with increased replication rates and expanded cell tropism may similarly reflect reduced selection pressures in a declining immune state (10, 75, 81) and adaptation to the use of different coreceptor molecules (85).

Studies of HIV-1 evolution within individuals with different rates of disease progression have been limited by the large-scale DNA sequencing required to analyze complex quasispecies. Genetic analyses have demonstrated the homogeneity of envelope sequences immediately following homosexual transmission as well as following mother-infant, and parenteral transmission (15, 61, 87, 90, 92). Variable rates of replacement of viral variants have also been noted (37, 53, 78). Cross-sectional analysis of samples from individuals at different stages of disease (15, 17) or longitudinal studies involving small numbers of patients (15, 21, 37, 49, 53, 65, 86, 88, 89) have examined possible links between quasispecies diversity, rate of sequence change, and disease progression. It was proposed, based on theoretical grounds and HIV-1 sequences derived from two individuals, that AIDS results from an inability of the immune system to control more than a threshold level of HIV-1 variants (56–58). However, complex quasispecies were detected in asymptomatic adults and children while limited viral heterogeneity was detected in very rapid progressors (15,

* Corresponding author. Mailing address: Aaron Diamond AIDS Research Center, 455 First Ave., New York, NY 10016. Phone: (212) 725-0018. Fax: (212) 725-1126. E-mail: delwart@adarc.org.

21, 40, 78, 86, 89). Similarly, high levels of genetic diversity in simian immunodeficiency virus did not appear to correlate with disease progression (27).

To test the hypothesis that the rate of HIV-1 evolution is a function of host selective forces imposed on the replicating quasispecies, changes in proviral envelope genes were analyzed by using a larger set of samples and individuals than previously analyzed. Longitudinal changes in viral populations within individuals were compared to rates of $CD4^+$ cell decline and levels of plasma viremia. In this study, the development of quasispecies diversity, clearance of the earliest detected variants, the representation in vivo of the variants replicating in short-term PBMC cocultures, and the genetic differences between complex quasispecies present at later stages of infection were determined by DNA heteroduplex mobility assays (HMA) and heteroduplex tracking assays (HTA) (15, 16). HIV-1 evolution was generally faster in individuals retaining high $CD4^+$ cell levels than in either rapidly progressing or severely immunocompromised patients.

MATERIALS AND METHODS

Patient information and samples. Patients were selected from the San Francisco Men's Health Study cohort (75). Starting in 1984, blood samples were collected every 6 months from enrolled volunteers and tested for HIV-1 seropositivity. Eleven individuals who seroconverted after entry into the cohort and exhibited widely different rates of $CD4^+$ cell decline were selected according to sample availability. PBMC samples obtained 6 months prior to the first seropositive samples were also tested by PCR for HIV-1 env DNA as described previously (16). Initially PCR-positive (time zero) samples for seroconverters were therefore obtained within 6 months of primary infection. To study the later phase of infection in more detail, six individuals already seropositive at cohort entry, five of whom progressed to AIDS during the period studied, were also included in this study. Efforts were made, depending on sample availability, to analyze samples collected throughout the course of infection, including the earlier available HIV-1 DNA-positive sample for seroconverters and the last sample available before death for progressors. Plasma viral RNA loads were determined by QC-PCR (55). The syncytium- or non-syncytium-inducing phenotypes of PBMC cocultured viral isolates were determined by an MT-2 syncytium assay (75).

PCR, HMA, and HTA. DNA was extracted from uncultured and cocultured PBMCs, and a 700-bp fragment spanning the third through fifth variable regions (V3 through V5 regions) of env was amplified by a nested-PCR (nPCR) protocol able to amplify a single provirus in 1.5×10^5 cells, as previously described (16). In order to appropriately sample the complex quasispecies seen in vivo, measures were taken to ensure the analysis of multiple variants from each proviral population. A semiquantitative determination of proviral load was performed by duplicate 5- or 10-fold end-point limiting dilution of the PBMC DNA prior to nPCR. A positive nPCR, indicating the presence of at least one HIV-1 provirus, was used to estimate the number of amplified genomes in 1 μg of DNA. A minimum of 20 proviral genomes were analyzed from each quasispecies. When a low proviral load precluded the amplification of at least 20 genomes from 1 μg of PBMC DNA, the amplified DNA from multiple independent nPCRs were pooled before further analysis. Heteroduplexes formed between divergent env sequences were separated on 5% polyacrylamide gels (acrylamide/bis ratio, 30:1) at 250 V for 2.5 h. Gels were stained with ethidium bromide (0.5 μg/ml) and UV illuminated, and the image was recorded with a charge-coupled device (CCD) camera (UVP, Upton, Calif.). HTA employed a single-stranded DNA probe generated with a 5′-biotinylated primer (ES7) (16) and a 5′-³²P-labeled (by using T4 kinase) primer (ES8) (16) in the second PCR round. After PCR, the labeled DNA was bound to streptavidin-coated magnetic beads (Dynal, Lake Success, N.Y.). Magnetic beads were washed according to the manufacturer's recommendations, and the labeled strand was disassociated with 8 μl of 0.1 N NaOH for 10 min. The probe was neutralized by adding 40 μl of H_2O, 4 μl of 0.2 N HCl, and 1 μl of 1 M Tris-HCl (pH 7.4). The probe (5,000 cpm; typically 0.3 μl) was reannealed with approximately 250 ng of target DNA from second-round PCR DNA (5 μl) by heating the probe-target mixture to 94°C for 1 min and rapidly cooling it to room temperature in a thermocycler. Heteroduplexes were resolved on polyacrylamide gels as described above. When a single-stranded probe is used, each radiolabeled heteroduplex band reflects hybrid formation with one or more unique variant in the target quasispecies. Vacuum-dried gels were used to expose a PhosphorImager plate (Molecular Dynamics, Sunnyvale, Calif.) for signal detection and quantitation.

Data analysis. Images from HMA gels were captured with a CCD camera and stored as binary TIFF files. Gel lanes were scanned by using the plot profile function of the NIH Image 1.56b freeware analysis package. Lane scans within the same gel were of equal length (same number of pixels) and recorded from positions immediately below the single-stranded DNA position to immediately

below the homoduplex. The signal intensity at each pixel along the scan was transferred to a Microsoft Excel (Richmond, Wash.) file. The quasispecies diversity for each sample was estimated by using a normalized Shannon entropy (18, 34, 38, 73, 89) measurement of each HMA gel lane. Since different numbers of pixels per lane were acquired from different gels, each gel was standardized by partitioning into 137 divisions, the smallest number of pixels in the scans under study. This allowed the maximum distinction of fine banding patterns, while permitting unbiased comparisons between gels. The Shannon entropy (S) is defined by the following formula: $S = -\Sigma$ (from $i = 1$ to N) $P(i)\ln[P(i)]$, where N is the number of partitions in a lane, and $P(i)$ is the fraction of the total signal in partition i. The maximum possible entropy is $\ln(N)$, and we defined the normalized entropy as $S/\ln(N)$. The normalized entropy has a range of 0 to 1, where 0 reflects no diversity (all of the signal is in a single partition), and 1 reflects maximum entropy, in which the signal is evenly distributed throughout all partitions in the lane.

Median mobility shift (MMS) values were derived by adding the signal intensity at each pixel along a lane starting from the bottom of the scan until they reached 50% of the total value of all pixels in that lane. That pixel position was divided by the total number of pixels in the lane to derive the MMS value.

For HTA, quantitative scans of the radioactivity distributed along the length of gel lanes were made by using the Molecular Dynamics ImageQuant program, and the data for each pixel were transferred to Excel files. Lane scans within the same gel were of equal length (same number of pixels) and recorded from immediately below the single-stranded DNA position to immediately below the homoduplex. The difference between the signal distribution of the lane displaying the quasispecies homologous to the probe (k) and neighboring lanes (j) on the same gel were calculated as follows. The radioactive signal in each lane j was converted into a probability distribution, $P_{-j}(i)$, as was done for the HMA diversity measurements. The sum of the values for each lane was normalized to equal 1 to account for slight differences in the amount of probe. Then, to take into account imprecision in the scan (and therefore in the associated probability distribution) each probability distribution was convolved with a Gaussian distribution whose width was 1.5% of the number of pixels in the lane. This slight correction was arbitrarily chosen to account for gel smile effects during the electrophoretic run on the mobility of bands. Each distribution was therefore slightly smoothed, so that any experimental noise-induced differences between identical lanes would be reduced. The absolute value of the difference (between the lanes' associated probability distributions) at each lateral pixel position was calculated. These differences were then summed over all such pixels to yield the final absolute difference value in the signal distribution between lanes. When comparing two HTA lanes on the same gel, the absolute difference measure between lane j and lane k was therefore calculated as follows: $D_{jk} = \Sigma$ (from $i = 1$ to N) $|P_j(i) - P_k(i)|$. Identical lanes therefore produced an absolute value of $D = 0$, while completely nonoverlapping signal distributions between two lanes resulted in an absolute difference value of $D = 2$. Reconstitution experiments with known amounts of different variant DNAs showed that the fraction of the total radioactive signal with homoduplex mobility directly reflected the fraction of target DNA homologous to the single-stranded HTA probe (data not shown). The percentage of the quasispecies comigrating and therefore similar to the probe ($D = 2$) to 100% ($D = 0$).

For Fig. 1, images from the CCD camera and PhosphorImager were converted to 8-bit TIFF files, opened in Photoshop 3.0 (Adobe Systems, Mountain View, Calif.), and transferred to the graphics program Canvas 3.53 (Deneba Systems, Miami, Fla.).

Correlation coefficients (r) and probability values (P) were determined by linear regression (Microsoft Excel 5.0).

DNA sequence analysis. Single proviral env molecules derived by end point dilution of uncultured PBMC DNA were amplified by nPCR and directly sequenced as previously described (15, 76, 77). In one case (P349), sequence quality was not adequate and sequences were therefore determined from three plasmid subclones. V3 to V5 sequences were aligned by using PILEUP (22) and CLUSTAL W (82), and the numbers of different bases in pairwise comparisons were determined by using MEGA (39) after removing nonalignable regions of length variation in V4 and V5. Phylogenetic analysis was performed by the neighbor-joining method (71) with a sequence matrix determined by the two-parameter method of Kimura (31). Bootstrap support was determined with 1,000 resamplings of the sequences as implemented in the PHYLIP package.

RESULTS

Rapid $CD4^+$ cell count decline correlates with higher levels of viremia. Eleven individuals whose primary infection could be timed within a 6-month window and who exhibited a broad range of disease progression rates were selected for this study. Rates of $CD4^+$ cell decline and time of death from AIDS were used to group these patients into three categories (Fig. 1A and B). Three individuals classified as rapid progressors (identification numbers beginning with RP) underwent precipitous $CD4^+$ cell count decline and died of AIDS within 3 years of
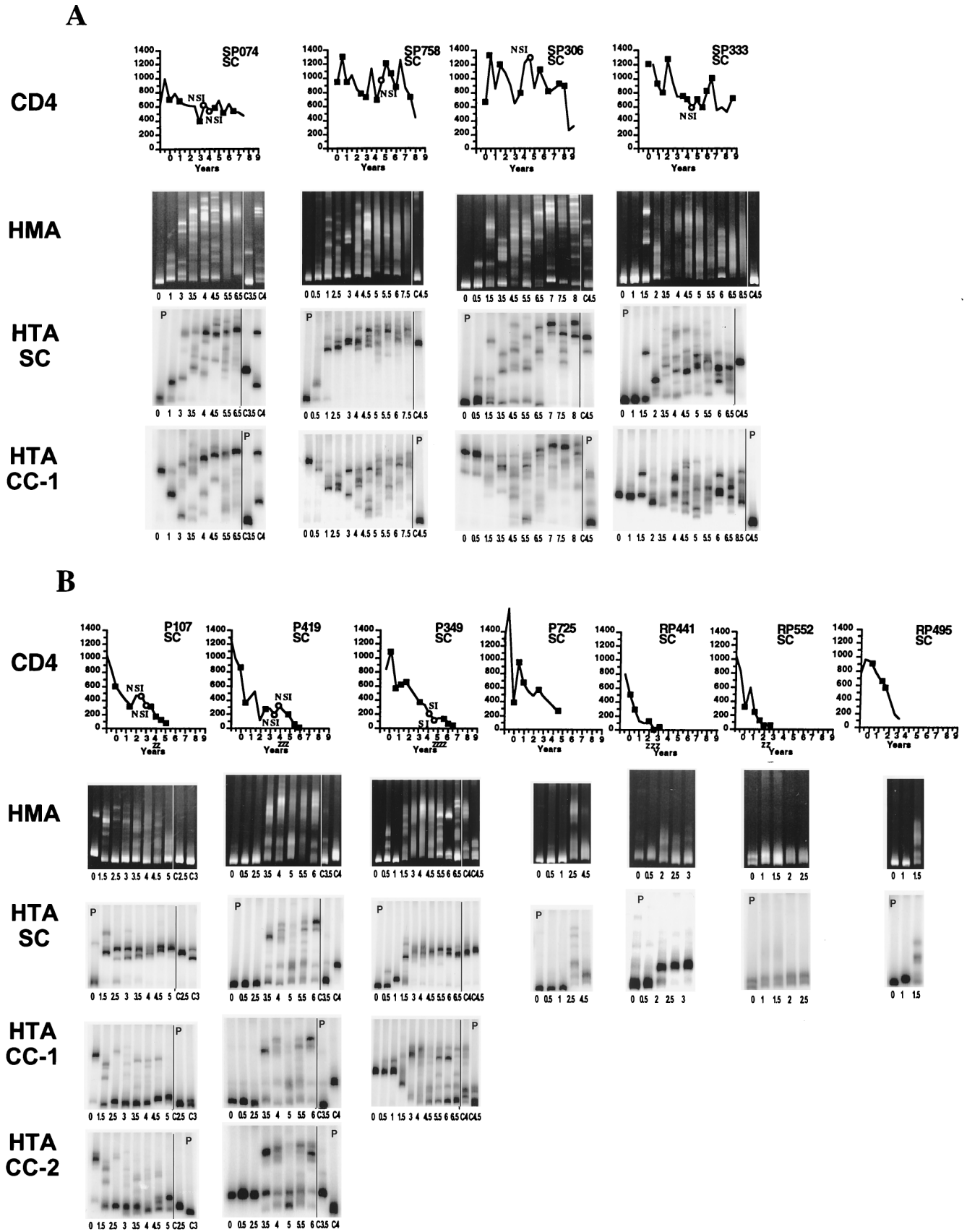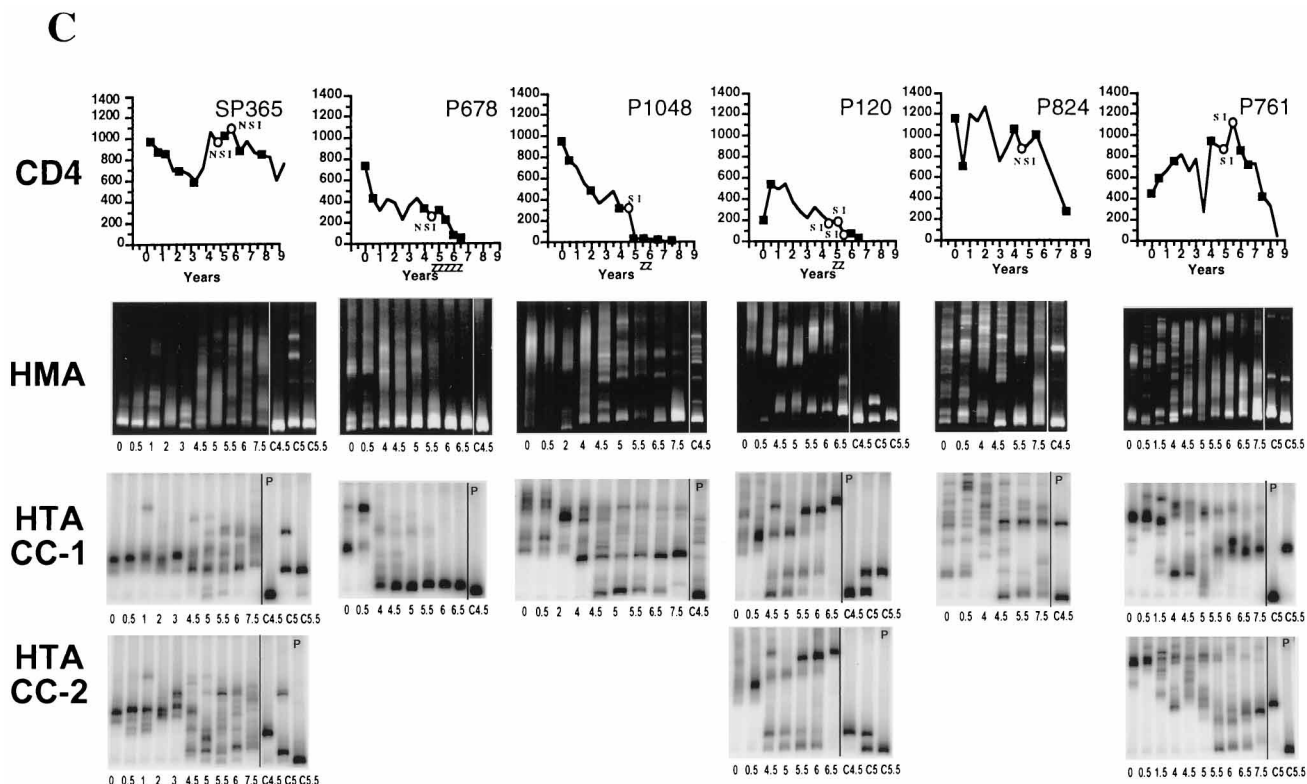
FIG. 1. CD4+ cell counts, HMA, and HTA. Patient identification numbers are indicated in the top row of each panel. See Results for criteria pertaining to progression rates. SC indicates a person (seroconverter) infected <6 months prior to the first time point. The letter Z below the year (x axis) indicates time of AZT

monotherapy. The phenotypes of the cocultured isolates (syncytium inducing [SI] or non-syncytium inducing [NSI]) are indicated next to the PBMC time point from which they were derived. (A) Slow-progressing seroconverters; (B) progressors and rapid-progressing seroconverters; (C) individuals already infected at cohort entry. The uncultured PBMC samples analyzed in the accompanying gels are shown by solid squares and open circles. PBMC samples also used to derive coculture variants are shown by open circles. HMA indicates ethidium bromide-stained polyacrylamide gels. HTA SC indicates the HTA patterns for seroconverters with the earliest HIV-1-positive sample used as the probe. HTA CC indicates the HTA patterns with one (CC-1) or a later-derived (CC-2) coculture variant used as the probe. P on the HTA gels indicates the sample used to generate the single-stranded HTA probes. Gel images are shown below the single-stranded DNA mobility positions, to which all of the intrapatient heteroduplexes migrate. Lines are used to separate uncultured PBMC from the cocultured virus isolate variants. No virus isolates were available for P725 and the rapid progressors. Lanes labeled with numbers only contain uncultured PBMC proviral variants from the indicated years; lanes beginning with C contain cocultured proviral variants.

infection (RP441, RP495, and RP552). Four individuals classified as progressors (identification numbers beginning with P) experienced a less-steep CD4$^+$ cell decline and died of AIDS 5 to 7 years postinfection (P107, P349, P419, and P725). Four individuals classified as slow progressors (identification numbers beginning with SP) remained asymptomatic 8 years postinfection, with an average final CD4$^+$ cell count of 527/μl of blood (range, 319 to 722) (SP074, SP306, SP333, and SP758). Another six individuals infected prior to entry into the cohort study and whose rates of progression relative to primary infection are therefore unknown were also chosen (Fig. 1C). Four of these individuals died of AIDS 6.5 to 7.5 years after study entry (P120, P678, P824, and P1048), one subject underwent a CD4$^+$ cell count decline to <20 CD4$^+$ cells/μl of blood 8.5 years after study entry (P761), and one subject remained asymptomatic, with a CD4$^+$ cell count of >600 (SP365) 9 years after study entry.

Longitudinal plasma viral RNA loads were determined for 10 of the 11 seroconverters (Fig. 2). Some individuals showed a greater-than-10-fold drop in plasma viremia immediately after the first HIV-1-positive sample. Seroconverters classified as slow progressors then sustained lower viral loads than did progressors and rapid progressors. Average plasma viral RNA loads, starting from the second PCR-positive sample, were 1.5 × 10^4, 5.6 × 10^4, and 2.2 × 10^5 HIV-1 RNA molecules/ml of plasma for slow progressors, progressors, and rapid progres-

sors, respectively. In order to test for correlation between rates of disease progression and plasma viral loads, the CD4$^+$ cell count slopes were determined for seroconverters starting 6 months before the first PCR-positive bleed and continuing until the last sample was collected (Fig. 1A and B). A positive correlation was seen between steeper CD4$^+$ cell count slopes and higher average viral loads (r = 0.9; P = 0.0002). The highest single plasma viral RNA load measured (1.1 × 10^6 HIV-1 RNA molecules/ml of plasma) was found preseroconversion in P725, and it preceded the steepest CD4$^+$ cell count drop in a 6-month period (decline of 1,340 cells/μl of blood) (Fig. 1B, P725).

Faster CD4$^+$ cell count decline correlates with slower viral genetic diversification. Proviral DNAs from a total of 135 PBMC samples were analyzed, starting with those from the first PCR-positive visit for seroconverters (n = 11) or those taken at cohort entry for seroprevalent subjects (n = 6). Subjects were monitored for up to 8.5 years or until death from AIDS. DNA was extracted, and a 700-bp region, including the V3 through V5 regions of the HIV-1 envelope gene, was amplified by nPCR.

HMA was used to estimate the level of genetic diversity within each quasispecies. Divergent *env* sequences simultaneously amplified by nPCR were randomly reannealed to form heteroduplexes which were then resolved on 5% polyacrylamide gels, stained with ethidium bromide, and visualized after
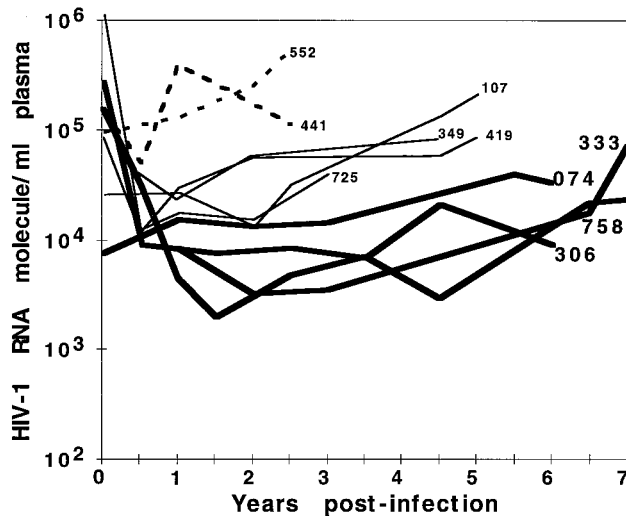
FIG. 2. Longitudinal plasma viral loads of 10 seroconverters. Slow progressors, progressors, and rapid progressors are shown with thick, thin, and dashed lines, respectively. Patient identification numbers are indicated.

UV illumination. In this assay, the various coamplified *env* variants form heteroduplexes whose reduced electrophoretic mobilities are influenced by the exact sequences of the mismatched and unmatched nucleotides in their distorted DNA double helix. HMA patterns for each individual over time are shown in Fig. 1. The initial proviral *env* quasispecies in 9 out of 11 seroconverters (Fig. 1A and B) appeared genetically homogeneous, as reflected by the presence of a single, fast-migrating DNA homoduplex band. In two seroconverters (P107 and RP552), two variants were detected in the first PCR-positive blood collection. Since seroconverters were analyzed up to 6 months after primary infection, the early variants detected in P107 and RP552 may have descended from an earlier homogeneous quasispecies or two divergent variants may have been transmitted. Genetic diversity subsequently increased in all seroconverters, as determined by the appearance of multiple heteroduplexes with reduced mobilities (Fig. 1A and B).

The possibility that the rate of increase in diversity of the viral population was a function of selection pressures imposed by the host and inversely correlated with the rate of disease progression was examined by image analyses of the DNA HMA patterns by two methods. Genetic diversity was first estimated by an analytical method based on the complexity or spread (Shannon entropy) of the signal distribution within each HMA gel lane (Materials and Methods). This measurement gave the lowest value to a single band (as seen early in infection) and increasing values for lanes with increasing numbers of heteroduplex bands. The diversity measure derived by this method was highest in lanes containing broad smears of heteroduplexes (rather than distinctive bands), indicating the presence of a highly differentiated quasispecies without dominant variants. The resulting diversity measures were plotted against time starting from the first HIV-1-positive sample (Fig. 3A). The two seroconverters with the fastest rate of progression to AIDS (RP441 and RP552) retained nearly homogeneous quasispecies, indicating that progression to AIDS could take place prior to the generation of a highly complex quasispecies (Fig. 1B and 3A). P419 also retained a homogeneous *env* population for 2.5 years, while his $CD4^+$ cell count dropped to 270. The four slowly progressing seroconverters rapidly evolved and then maintained genetically complex qua-

sispecies (Fig. 1A and 3A). Since all of the earliest postinfection samples exhibited low diversity (Fig. 3A), no correlation was found between quasispecies diversity values at time zero and the subsequent slope of $CD4^+$ cell decline ($r = 0.074$, $P = 0.83$). However, when the average diversity of the samples taken 0.5 and 1 year postinfection was plotted against the overall $CD4^+$ cell count drop per year, a correlation was found between maintenance of low viral diversity and faster $CD4^+$ decline ($r = 0.72$, $P = 0.017$). This correlation also held when the average of diversity values from 0.5 to 3 years postinfection was used ($r = 0.69$; $P = 0.017$) (Fig. 3B). This trend was especially clear for two of the three most rapid progressors (RP441 and RP552) (Fig. 1B and 3A). A slower initial increase in genetic diversity was therefore correlated with a steeper $CD4^+$ cell decline.

The above-described diversity measure was based on the pattern of distribution of heteroduplexes in HMA rather than on their specific electrophoretic mobilities. Because the mobility shift of heteroduplexes through polyacrylamide gels is proportional to the sequence difference between the reannealed DNA strands (14–16), the MMS of heteroduplexes was also used to estimate the degree of divergence between the variants present within quasispecies (Materials and Methods). MMSs found for seroconverters are plotted in Fig. 3C. Two years after infection, the smallest MMSs were found in RP552, RP441, and P419, indicating the maintenance of proviral populations with low levels of diversity. As expected, no correlation was found between the MMS at the initial time point and the $CD4^+$ slope ($r = 0.23$, $P = 0.486$). However, when the average of the MMSs determined from the samples available from 0.5 and 1 year was plotted against the $CD4^+$ slope, a weak correlation between smaller MMS and faster $CD4^+$ cell count decline was detected ($r = 0.57$, $P = 0.081$). This correlation improved when the average MMSs from 0.5 to 3 years postinfection were examined ($r = 0.673$; $P = 0.02$) (Fig. 3D). Again, this trend was especially clear for two of the three most-rapid progressors (RP441 and RP552) (Fig. 1B and 3C). Median mobilities therefore substantiated the visual observations and entropy-based diversity measurements, indicating that quasispecies with initially low rates of diversification were more likely to be found in rapid progressors versus slow progressors.

Reduction in quasispecies diversity late in disease progression. Quasispecies diversity was also quantified in six other individuals who entered the cohort already seropositive, all but one of whom progressed to AIDS over the period studied. A decrease in quasispecies diversity by the entropy measure was observed in three of five progressors (P120, P678, and P1048) late in their disease course, when $CD4^+$ cell numbers approached or were maintained near zero (Fig. 1C and 3E). Reduction in intraquasispecies sequence divergence late in disease progression was also seen for the same patients when the MMS measure was used (Fig. 3F). PBMC samples collected within 6 months prior to death from 7 of 10 AIDS patients showed low proviral diversity (entropy, <0.8), while the last sample tested from 5 of 5 individuals who retained high $CD4^+$ counts showed high diversity (entropy, >0.8) (Fig. 3A and E). Similar results were observed with MMS values, with 9 of 10 individuals tested 6 months prior to death from AIDS showing low intraquasispecies sequence divergence (MMS, <0.4), while the last sample tested from 5 of 5 individuals who retained high $CD4^+$ counts showed high intraquasispecies diversity (MMS, >0.4) (Fig. 3C and F). Low genetic diversity immediately prior to death from AIDS was therefore due both to the retention of relatively homogeneous quasispecies from early infection onward in some of the rapid and regular progressors and to the late emergence of low-complexity (clonal)
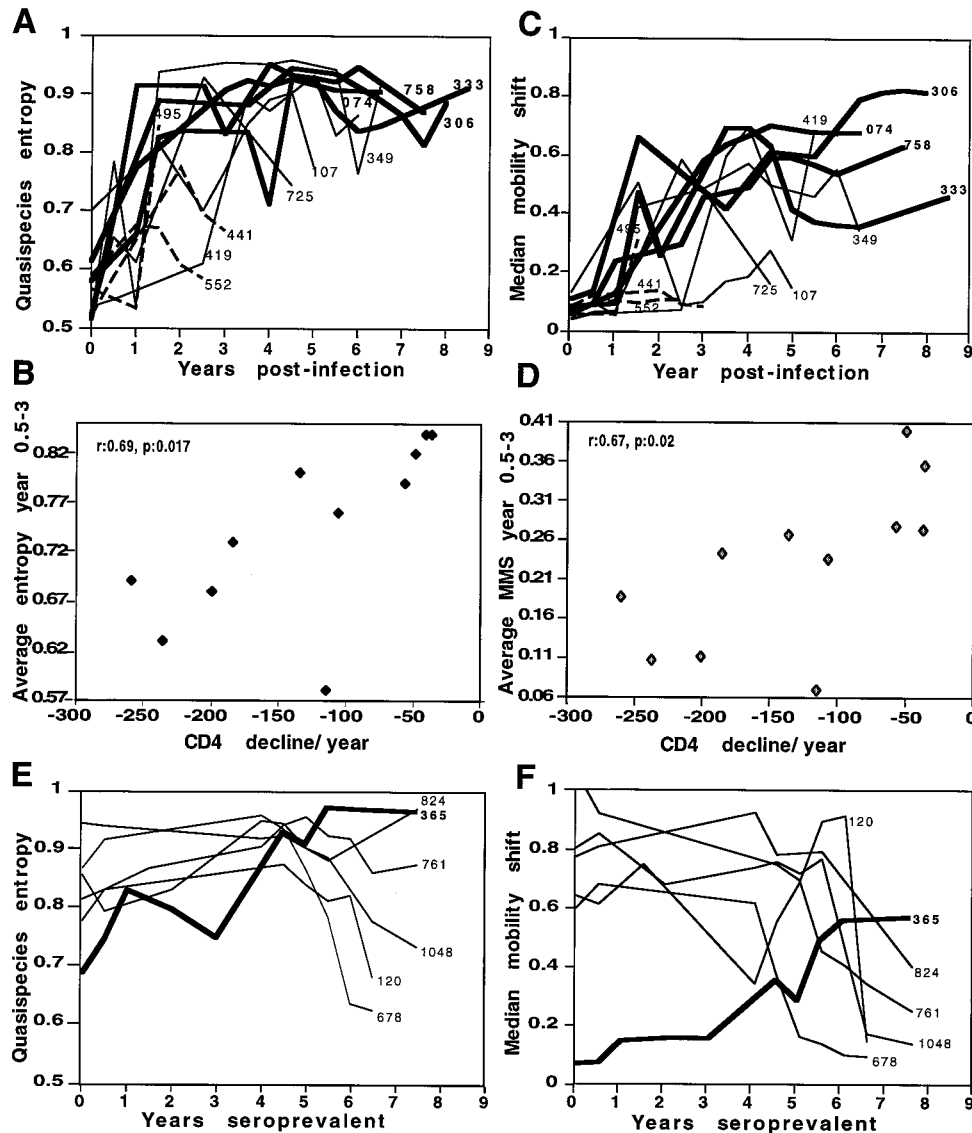
FIG. 3. Quasispecies diversification. (A) Quantitation of quasispecies diversity for the 11 seroconverters, using entropy measurements of HMA signal distribution; (B) rates of CD4^{+} cell decline per year and average of entropy values for samples collected from 0.5 to 3 years postinfection; (C) quantitation of intraquasispecies divergence, using median heteroduplex mobility shifts for all 11 seroconverters; (D) rates of CD4^{+} cell decline per year and average MMSs for samples collected from 0.5 to 3 years postinfection; (E) estimated quasispecies diversities for the five progressors and one slow progressor already infected at cohort entry, using entropy measurements of HMA signal distribution; (F) MMSs for the five progressors and one slow progressor already infected at cohort entry. Data from slow progressors, progressors, and rapid progressors are shown with thick, thin, and dashed lines, respectively. Patient identification numbers are indicated (A, C, E, and F).

variant populations from more-complex viral populations in other progressors (P107, P120, P678, P725, and P1048) (Fig. 1B and C and Fig. 3).

The replacement rate of the early strain is highly variable. The representation of specific variants within quasispecies was determined by HTA. Tracer amounts of single-stranded radio-labeled probe from specific variants were generated and then reannealed with a large excess of unlabeled DNA from target quasispecies (Materials and Methods). Under these conditions, the single-stranded HTA probe and target DNA formed radiolabeled DNA heteroduplexes whose precise mobilities were sequence specific, reflecting the genetic relationship between the probe and target sequence variants. The fraction of radiolabeled signal migrating with the mobility of homodu-

plexes reflected the proportion of variants in the target DNA that was genetically closely related to the probe variants.

HTA was first used to determine whether the earliest appearing variants were replaced by divergent genomes at different rates depending on the rate of progression to AIDS. Single-stranded HTA probes were generated from virus found within 6 months of infection from seroconverters and reannealed to target DNA from subsequent time points. The replacement of the initial variant population by divergent sequences is visualized in Fig. 1A and B in the gels marked HTA SC. The overlap in signal distribution was calculated between the time zero control lane (where both probe and target populations were the same) and the lanes containing target PBMC DNA from later samples. The extent of signal distribution
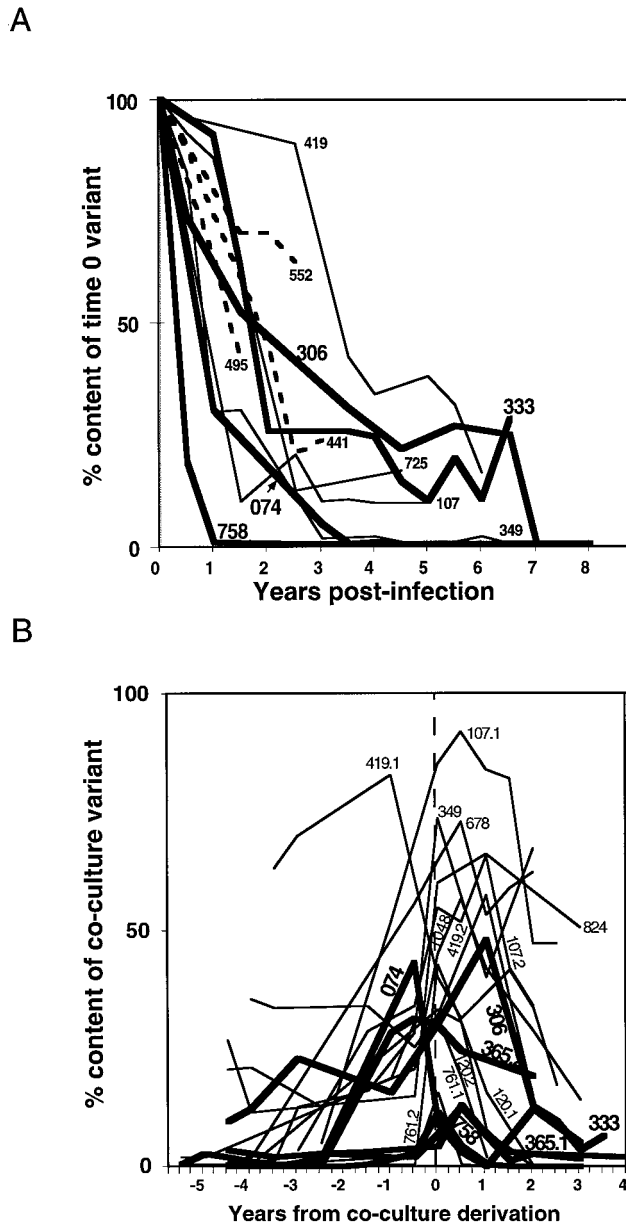
A

B

FIG. 4. Representation of the initial and cocultured variants as PBMC proviruses over time. (A) Replacement of the initial variant by divergent genomes. With the earliest PCR-positive specimen as the HTA probe, the difference between the initial HTA pattern and that from later PBMCs was used to determine the percentage of the initial variant in later quasispecies of 11 seroconverters. (B) Representation of cocultured variants in PBMC proviral DNA. With proviral DNA from cocultures as the HTA probes, the difference between the HTA patterns derived with cocultured and uncultured proviral DNAs as target was used to determine the percentage of cocultured variants in vivo over time. Time zero was the time point from which the cocultures used as probes were derived from PBMC samples. Patient identification numbers are indicated. When two different cocultures were used as probes, the results obtained with the earlier derived coculture probe end with .1 and those derived with the later one end with .2. Data from slow progressors, progressors, and rapid progressors are shown with thick, thin, and dashed lines, respectively.

overlap was then used to determine the percentage of the variants in vivo that were closely related to the HTA probe variants (Materials and Methods). A highly variable rate of replacement of the early variant population was observed (Fig. 4A). In some seroconverters, replacement was almost com-

plete within 2 years (SP074, SP758, SP333, P107, and P349). P419 retained detectable levels of his initial variant until his death 6 years later. Early variants were also retained in SP306 for 6.5 years (Fig. 1A and 4A). After 2.5 years of infection, variants in RP552 showed slightly reduced heteroduplex mobilities (Fig. 1B), indicating the accumulation of minor genetic changes. In RP441, the proviral population made a single shift to a new variant form between 0.5 and 2.5 years postinfection (Fig. 1B). Overall, no significant correlation was seen between the rate of CD4^{+} decline and the rate of replacement of the initial variant during the early years of infection.

Representation and genetic turnover of coculture-like proviruses in vivo. Viral evolution was also analyzed later in the course of infection when CD4^{+} cells had significantly declined in some subjects. In order to determine the representation of at least a fraction of the replication-competent variants present in vivo, the viruses amplified by short-term PBMC coculture were used as HTA probes. Patient PBMCs (10^6) were cultured for 7 to 28 days with uninfected phytohemagglutinin-activated PBMCs (75), and the cellular DNA was extracted from p24 supernatant-positive cocultures. Proviral DNA in these cocultures generally appeared to be homogeneous by HMA (Fig. 1, lanes labeled C on the right sides of the gels). To assess the in vivo representation of variants that replicated in tissue culture, single-stranded HTA probes were generated from the proviral DNA in cocultured cells and reannealed with target DNA from uncultured PBMCs. The differences between the signal distribution in the lane in which the probe was reannealed to the homologous cocultured variants and those lanes where the target DNA consisted of proviral variants from uncultured PBMCs from different time points were determined. As described above, HTA signal distribution overlap was expressed as the relative representation of the coculture variants in the PBMCs (Fig. 4B) (Materials and Methods). This analysis indicated that variants amplified by cocultivation formed a larger fraction of the proviruses in the PBMCs from which they were derived in progressors than in those of slow progressors (Fig. 4B, dashed line). Cocultured isolate variants were therefore more representative of the proviral quasispecies in vivo for progressors than for slow progressors. Variants closely related to those in coculture also persisted in vivo for longer periods in progressors than in slow progressors (Fig. 4B). This could also be visualized by the persistence of the homoduplex mobility signal when uncultured PBMC variants from progressors were probed with cocultured variants (Fig. 1B and C, HTA CC gels). Uncultured PBMC variants from slow progressors showed a characteristic V-shaped HTA pattern when probed with cocultured variants, reflecting the replacement of the coculture-like variants in vivo by divergent genomes (Fig. 1A, HTA CC gels). Progressors also showed the long-term persistence of variants other than those related to the coculture variants, as reflected by strikingly similar overall heteroduplex patterns in adjacent lanes (Fig. 1B and C, HTA CC gels). Slow progressors therefore displayed different HTA patterns at adjacent time points throughout their asymptomatic infection (Fig. 1A, HTA CC gels), whereas a fixation of the HTA pattern appeared to take place in progressors late in their disease progression (Fig. 1B and C, HTA CC gels). The evolution of the proviral quasispecies as a whole therefore appeared more static in patients with low CD4^{+} cell counts than in individuals retaining high CD4^{+} cell counts.

Progressors P761 and P824 both underwent steep CD4^{+} cell count declines after prolonged periods of stable, high CD4^{+} cell levels (Fig. 1C). Plasma viral load rose >100-fold during this period, reaching the range observed in the rapid progressors (increasing from 10^3 to 2×10^5 RNA molecules/ml of
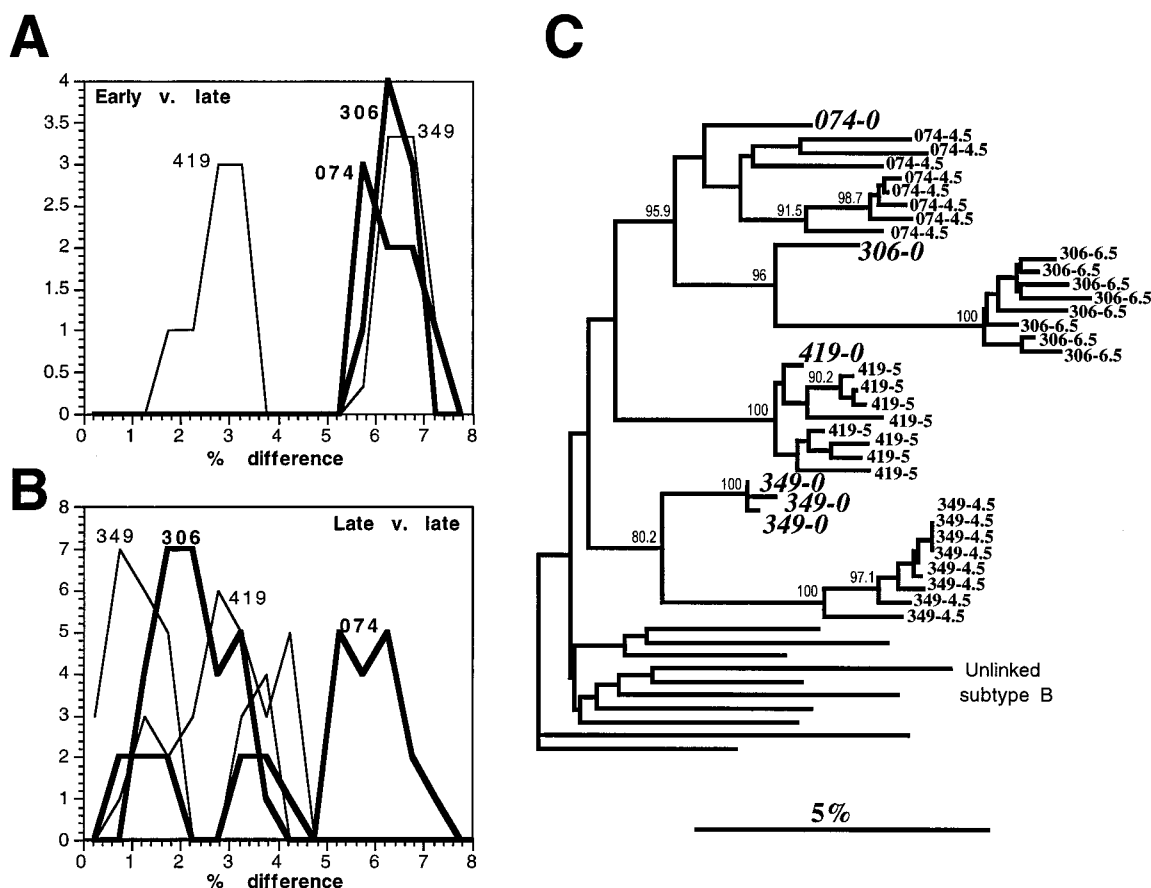
FIG. 5. DNA sequence analysis of the V3 to V5 region of *env* from four individuals. Numbers of pairwise alignments between the initial and later variants (A) and among the later variants (B) are shown, both with their percent nucleotide difference. (C) Neighbor-joining phylogenetic tree showing patient clusters and distances between variants. The numbers at the nodes define instances of support in >75% of 1,000 bootstrap resampling. Data from slow progressors and progressors are shown with thick and thin lines, respectively.

plasma between year 5 and 8.5 for P761 and from <500 to 7 × 10^4 RNA molecules/ml of plasma between year 4.5 and 7.5 for P824). As did the more regular progressors, P824 maintained proviruses in vivo during his sharp $CD4^+$ cell count drop that were highly related to the cocultured variants (Fig. 1C and 4B). PBMC proviruses in P761 were probed with virus from two different cocultures. With the cocultured variant derived 6 months before the beginning of the $CD4^+$ cell count drop as the HTA probe, only low levels of closely related proviruses were detected in vivo. With a PBMC coculture probe derived immediately prior to the $CD4^+$ cell count decline, closely related variants were detected at higher levels and were maintained in vivo for 1 year (Fig. 1C and 4B). These data suggest that a sudden decline in $CD4^+$ cell count may also be associated with abundant representation of variants capable of replicating in vitro and their perpetuation in vivo over time with fewer genetic changes than are seen in the context of sustained CD4 cell counts.

DNA sequence analysis. *env* V3 to V5 variants derived by end point dilution of PBMC DNA from four individuals (SP074, SP306, P349, and P419) were amplified by nPCR and directly sequenced (15, 76). A single variant (or three subclones, in the case of P349 [Materials and Methods]) from the homogeneous populations present at the first positive time point and eight variants from the viral populations collected 4.5 to 6.5 years later were analyzed. The percent nucleotide

differences between aligned sequence variants and the initial variant as well as among later variants were calculated (Fig. 5A and B). The smallest number of mutations relative to the initial variant was found in P419 (Fig. 5A), whereas the most-diversified later population was found in SP074 (Fig. 5B), with similar levels of divergence found in patients SP306 and P349. Phylogenetic analysis confirmed these observations (Fig. 5C). An apparent linkage between the early variants in SP074 and SP306 is not unexpected for two men infected 1 year apart in the same town early in the U.S. epidemic (13). Hence, DNA sequence analysis results of proviruses in these four individuals were consistent with the trend of slower sequence changes in progressors (P419) and higher sequence diversification in slow progressors (SP074) as observed by heteroduplex analyses.

DISCUSSION

The genetic diversity of HIV-1 quasispecies at the *env* locus generally increased more slowly in progressors and rapid progressors than in slow progressors. Death from AIDS occurred prior to the development of a highly diverse quasispecies in two of the three most-rapid progressors (RP441 and RP552). These two patients also had the highest plasma viremia, and RP441 had one of the poorest anti-p24 antibody responses (data not shown). Thus, weak host-mediated selection, possibly due to poorly effective immune responses, may contribute to

the low levels of quasispecies diversification associated with high viremia and accelerated disease progression.

An antigenic threshold level has been postulated, above which complex quasispecies overwhelm the capacity of the immune system to suppress viral replication, resulting in progression to AIDS (57, 58). The rapid disease progression observed in the absence of extensive genetic diversification and the observation that slow progressors rapidly generated and then maintained highly diverse quasispecies without exhibiting profound CD4$^+$ cell depletion are inconsistent with a simple interpretation of this hypothesis. In a fraction of individuals a reduction in genetic diversity also occurred after extensive CD4$^+$ cell loss. The late outgrowth of a small number of variants in a subset of severely immunocompromised individuals resembles the viral diversity reduction observed during tissue culture amplification (15, 37, 40, 53) and as previously mentioned might be a consequence rather than a cause of profound immunosuppression (57).

The faster initial increase in quasispecies diversity measured by either entropy or median heteroduplex mobility in slow progressors indicates that a greater number of more-divergent genomes evolved from the initial variant in these individuals. Replacement of the initial variant by a divergent genome(s) occurred at highly variable rates, with even the fastest progressors (RP441 and RP552) showing gradual accumulation of minor genetic changes. While clearance of the initial variants did not correlate with progression rate, the overall greater number of variants (entropy) and levels of divergence between variants (MMS) indicated that a wider diversification of the quasispecies took place in slow progressors than in rapid and more-typical progressors.

As previously reported, PBMC coculture typically results in the outgrowth of genetically more-homogeneous virus populations than found as proviruses in vivo (Fig. 2) (15, 37, 40, 53). Tissue culture-amplified variants may have arisen from a subset of PBMCs actively producing virus at the time of blood collection and/or from latently infected cells activated in coculture. In vitro amplification may also result in the outgrowth of the fastest-replicating variant(s) from a larger pool of replication-competent viruses. Proviruses closely related to these coculture-amplified variants were found at higher levels in subjects who progressed to AIDS than in those who remained asymptomatic (Fig. 4B). In the context of depressed and rapidly falling CD4$^+$ cell counts, such variants were also perpetuated for years, whereas they were rapidly replaced by divergent genomes in individuals who retained high CD4$^+$ cell counts. Other sequence variants were also perpetuated for long periods in some progressors (P120, P349, P419, P824, and P1048), as indicated by similar overall HTA patterns in succeeding time points. The rate of genetic change of proviral quasispecies as a whole therefore appeared to be reduced in the context of severe immunodeficiency.

Seven of the progressors received zidovudine (AZT) monotherapy (Fig. 1). Reduction in quasispecies diversity occurred during AZT therapy for P349 and P678 but also occurred more then 1 year after drug withdrawal for P1048 and P120 and had no discernible effect on the proviral quasispecies diversity for P107 and P419. In agreement with previous reports, a decrease in envelope gene diversity, indicative of an effective population bottleneck, was not consistently observed following AZT monotherapy (42, 91).

As expected based on the work of Mellors et al. (51, 52), viral loads seemed to be established early after infection at higher levels in progressors versus slow progressors, with both groups showing gradually increasing viremia (Fig. 2). The >2-log increase in plasma viremia starting after >4.5 years of

infection in P761 and P824 occurred along with sharp drops in CD4$^+$ levels, suggesting that the factors setting viral load can change rapidly and further underlining the temporal linkage between high viremia and CD4$^+$ decline (10).

Novel methods of DNA heteroduplex mobility pattern analyses were used here to monitor changes in HIV-1 quasispecies composition. These approaches allowed a larger number of proviral variants per sample, a larger number of samples per patient, and a larger number of patients to be analyzed than in prior longitudinal studies of quasispecies diversity. In summary, reduced rates of viral quasispecies diversification were detected in rapid progressors relative to slower progressors, with DNA sequence analyses agreeing with trends identified by DNA heteroduplex analyses. These results are also consistent with those of prior DNA sequence studies showing greater diversification and higher dN/dS ratios in slow versus more-rapid progressors (15, 21, 45, 89). The late reduction of proviral diversity in a subset of progressors and the genetically more-static nature of quasispecies late in disease progression have not been previously reported and may reflect a collapsing immune system no longer able to exert strong selective pressures on the replicating quasispecies. Rapid quasispecies diversification and their constant evolution in slow progressors may reflect more-effective immune responses and associated selection pressure.

REFERENCES

1. **Albert, J., B. Abrahamsson, K. Nagy, E. Aurelius, H. Gaines, G. Nyström, and E. M. Fenyö.** 1990. Rapid development of isolate-specific neutralizing antibodies after primary HIV-1 infection and consequent emergence of virus variants which resist neutralization by autologous sera. AIDS **4:**107–112.
2. **Arendrup, M., C. Nielsen, J.-E. S. Hansen, C. Pedersen, L. Mathiesen, and J. O. Nielsen.** 1992. Autologous HIV-1 neutralizing antibodies: emergence of neutralization-resistant escape virus and subsequent development of escape virus neutralizing antibodies. J. Acquired Immune Defic. Syndr. **5:**303–307.
3. **Bonhoeffer, S., E. C. Holmes, and M. A. Nowak.** 1995. Causes of HIV diversity. Nature **376:**125.
4. **Borrow, P., H. Lewicki, X. Wei, M. S. Horwitz, N. Peffer, H. Meyers, J. A. Nelson, J. E. Gairin, B. H. Hahn, M. B. A. Oldstone, and G. M. Shaw.** 1997. Antiviral pressure exerted by HIV-1-specific cytotoxic T lymphocytes (CTLs) during primary infection demonstrated by rapid selection of CTL escape virus. Nat. Med. **3:**205–217.
5. **Burns, D. P. W., C. Collignon, and R. C. Desrosiers.** 1993. Simian immunodeficiency virus mutants resistant to serum neutralization arise during persistent infection of rhesus monkeys. J. Virol. **67:**4104–4113.
6. **Burns, D. P. W., and R. C. Desrosiers.** 1991. Selection of genetic variants of simian immunodeficiency virus in persistently infected rhesus monkeys. J. Virol. **65:**1843–1854.
7. **Cao, Y., L. Qin, L. Zhang, J. Safrit, and D. D. Ho.** 1995. Virologic and immunologic characterization of long-term survivors of human immunodeficiency virus type 1 infection. N. Engl. J. Med. **332:**201–208.
8. **Cheng-Mayer, C.** 1993. HIV-1 variation: consequences for disease progression and vaccine strategies. Trends Microbiol. **1:**353–355.
9. **Coffin, J. M.** 1995. HIV population dynamics in vivo: implications for genetic variation, pathogenesis, and therapy. Science **267:**483–489.
10. **Connor, R. I., H. Mohri, Y. Cao, and D. D. Ho.** 1993. Increased viral burden and cytopathicity correlate temporally with CD4$^+$ T-lymphocyte decline and clinical progression in human immunodeficiency virus type 1-infected individuals. J. Virol. **67:**1772–1777.
11. **Deacon, N. J., A. Tsykin, A. Solomon, K. Smith, M. Ludford-Menting, D. J. Hooker, D. A. McPhee, A. L. Greenway, A. Ellett, C. Chatfield, et al.** 1995. Genomic structure of an attenuated quasi species of HIV-1 from a blood

transfusion donor and recipients. Science **270:**988–991.

12. **Dean, M., M. Carrington, C. Winkler, G. A. Huttley, M. W. Smith, R. Allikmets, J. J. Goedert, S. P. Buchbinder, E. Vittinghoff, E. Gomperts, S. Donfield, D. Vlahov, R. Kaslow, A. Saah, C. Rinaldo, R. Detels, and S. J. O'Brien.** 1996. Genetic restriction of HIV-1 infection and progression to AIDS by a deletion allele of the CKR5 structural gene. Science **273:**1856–1862.

13. **Delwart, E. L., M. P. Busch, M. L. Kalish, J. W. Mosley, and J. I. Mullins.** 1995. Rapid molecular epidemiology of HIV-1 transmission. AIDS Res. Hum. Retroviruses **11:**1181–1193.

14. **Delwart, E. L., B. L. Herring, A. G. Rodrigo, and J. I. Mullins.** 1995. Genetic subtyping of human immunodeficiency virus using a heteroduplex mobility assay. PCR Methods Appl. **4:**202–216.

15. **Delwart, E. L., H. W. Sheppard, B. D. Walker, J. Goudsmit, and J. I. Mullins.** 1994. Human immunodeficiency virus type 1 evolution in vivo tracked by DNA heteroduplex mobility assays. J. Virol. **68:**6672–6683.

16. **Delwart, E. L., E. G. Shpaer, F. E. McCutchan, J. Louwagie, M. Grez, H. Rübsamen-Waigmann, and J. I. Mullins.** 1993. Genetic relationships determined by a heteroduplex mobility assay: analysis of HIV *env* genes. Science **262:**1257–1261.

17. **Donaldson, Y. K., J. E. Bell, E. C. Holmes, E. S. Hughes, H. K. Brown, and P. Simmonds.** 1994. In vivo distribution and cytopathology of variants of human immunodeficiency virus type 1 showing restricted sequence variability in the V3 loop. J. Virol. **68:**5991–6005.

18. **Eigen, M.** 1971. Selforganization of matter and the evolution of biological macromolecules. Naturwissenschaften **58:**465–523.

19. **Epstein, L. G., C. Kuiken, B. M. Blumberg, S. Hartman, L. R. Sharer, M. Clement, and J. Goudsmit.** 1991. HIV-1 V3 domain variation in brain and spleen of children with AIDS: tissue-specific evolution within host-determined quasispecies. Virology **180:**583–590.

20. **Fenouillet, E., N. Blanes, A. Coutellier, J. Demarquest, W. Rozenbaum, and J.-C. Gluckman.** 1992. Monitoring of antibodies against human immunodeficiency virus type 1 p25 core protein as prognostic marker. J. Infect. Dis. **166:**611–616.

21. **Ganeshan, S., R. E. Dickover, B. T. M. Korber, Y. J. Bryson, and S. M. Wolinsky.** 1997. Human immunodeficiency virus type 1 genetic evolution in children with different rates of development of disease. J. Virol. **71:**663–677.

22. **Genetics Computer Group.** 1994. Wisconsin sequence analysis package, version 8.0. Genetics Computer Group, Inc., Madison, Wis.

23. **Ho, D. D., A. U. Neumann, A. S. Perelson, W. Chen, J. M. Leonard, and M. Markowitz.** 1995. Rapid turnover of plasma virions and CD4 lymphocytes in HIV-1 infection. Nature **373:**123–126.

24. **Hogervorst, E., S. Jurriaans, F. de Wolf, A. van Wijk, A. Wiersma, M. Valk, M. Roos, B. van Gemen, R. Coutinho, F. Miedema, et al.** 1995. Predictors for non- and slow progression in human immunodeficiency virus (HIV) type 1 infection: low viral RNA copy numbers in serum and maintenance of high HIV-1 p24-specific but not V3-specific antibody levels. J. Infect. Dis. **171:**811–821.

25. **Huang, Y., W. A. Paxton, S. M. Wolinsky, A. U. Neumann, L. Zhang, T. He, D. Ceradini, Z. Jin, K. Yazdanbakhsh, K. Kunstman, D. Erickson, E. Dragon, N. R. Landau, J. Phair, D. D. Ho, and R. A. Koup.** 1996. The role of a mutant CCR5 allele in HIV-1 transmission and disease progression. Nat. Med. **2:**1240–1243.

26. **Itescu, S., P. F. Simonelli, R. J. Winchester, and H. S. Ginsberg.** 1994. Human immunodeficiency virus type 1 strains in the lungs of infected individuals evolve independently from those in peripheral blood and are highly conserved in the C-terminal region of the envelope V3 loop. Proc. Natl. Acad. Sci. USA **91:**11378–11382.

27. **Johnson, P. R., and V. M. Hirsch.** 1992. Genetic variation of simian immunodeficiency viruses in nonhuman primates. AIDS Res. Hum. Retroviruses **8:**367–372.

28. **Jurriaans, S., B. Van Gemen, G. J. Weverling, D. Van Strijp, P. Nara, R. Coutinho, M. Koot, H. Schuitemaker, and J. Goudsmit.** 1994. The natural history of HIV-1 infection: virus load and virus phenotype independent determinants of clinical course? Virology **204:**223–233.

29. **Kaslow, R. A., M. Carrington, R. Apple, L. Park, A. Munoz, A. J. Saah, J. J. Goedert, C. Winkler, S. J. O'Brien, C. Rinaldo, R. Detels, W. Blattner, J. Phair, H. Erlich, and D. L. Mann.** 1996. Influence of combinations of human major histocompatibility complex genes on the course of HIV-1 infection. Nat. Med. **2:**405–411.

30. **Keet, I. P. M., P. Krijnen, M. Koot, J. M. A. Lange, F. Miedema, J. Goudsmit, and R. A. Coutinho.** 1992. Predictors of rapid progression to AIDS in HIV-1 seroconverters. AIDS **7:**51–57.

31. **Kimura, M.** 1980. A simple method for estimating evolutionary rates of base substitutions through comparative studies of nucleotide sequences. J. Mol. Evol. **16:**111–120.

32. **Klein, M. R., C. A. van Baalen, A. M. Holwerda, S. R. Kerkhof Garde, R. J. Bende, I. P. Keet, J. K. Eeftinck-Schattenkerk, A. D. Osterhaus, H. Schuitemaker, and F. Miedema.** 1995. Kinetics of Gag-specific cytotoxic T lymphocyte responses during the clinical course of HIV-1 infection: a longitudinal analysis of rapid progressors and long-term asymptomatics. J. Exp. Med. **181:**1365–1372.

33. **Kodama, T., K. Mori, T. Kawahara, D. J. Ringler, and R. C. Desrosiers.** 1993. Analysis of simian immunodeficiency virus sequence variation in tissues of rhesus macaques with simian AIDS. J. Virol. **67:**6522–6534.

34. **Korber, B. T., R. M. Farber, D. H. Wolpert, and A. S. Lapedes.** 1993. Covariation of mutations in the V3 loop of human immunodeficiency virus type 1 envelope protein: an information theoretic analysis. Proc. Natl. Acad. Sci. USA **90:**7176–7180.

35. **Korber, B. T., K. J. Kunstman, B. K. Patterson, M. Furtado, M. M. McEvilly, R. Levy, and S. M. Wolinsky.** 1994. Genetic differences between blood- and brain-derived viral sequences from human immunodeficiency virus type 1-infected patients: evidence of conserved elements in the V3 region of the envelope protein of brain-derived sequences. J. Virol. **68:**7467–7481.

36. **Koup, R. A., J. T. Safrit, Y. Cao, C. A. Andrews, G. McLeod, W. Borkowsky, C. Farthing, and D. D. Ho.** 1994. Temporal association of cellular immune responses with the initial control of viremia in primary human immunodeficiency virus type 1 syndrome. J. Virol. **68:**4650–4655.

37. **Kuiken, C. L., J. J. de Jong, E. Baan, W. Keulen, M. Tersmette, and J. Goudsmit.** 1992. Evolution of the V3 envelope domain in proviral sequences and isolates of human immunodeficiency virus type 1 during transition of the viral biological phenotype. J. Virol. **66:**4622–4627.

38. **Kullback, S.** 1959. Information theory and statistics. Wiley and Sons, New York, N.Y.

39. **Kumar, S., K. Tamura, and M. Nei.** 1994. MEGA: molecular evolutionary genetics analysis software for microcomputers. Comput. Appl. Biosci. **10:**189–191.

40. **Kusumi, K., B. Conway, S. Cunningham, A. Berson, C. Evans, A. K. N. Iversen, D. Colvin, M. V. Gallo, S. Coutre, E. G. Shpaer, D. V. Faulkner, A. deRonde, S. Volkman, C. Williams, M. S. Hirsch, and J. I. Mullins.** 1992. Human immunodeficiency virus type 1 envelope gene structure and diversity in vivo and after cocultivation in vitro. J. Virol. **66:**875–885.

41. **Lee, T. H., H. W. Sheppard, M. Reis, D. Dondero, D. Osmond, and M. P. Busch.** 1994. Circulating HIV-1-infected cell burden from seroconversion to AIDS: importance of postseroconversion viral load on disease course. J. Acquired Immune Defic. Syndr. **7:**381–388.

42. **Leigh-Brown, A. L., and A. Cleland.** 1996. Independent evolution of the env and pol genes of HIV-1 during zidovudine therapy. AIDS **10:**1067–1073.

43. **Lineberger, D. W., J. A. Kessler, J. A. Waterbury, V. W. Byrnes, F. Massari, S. Staszewski, and E. A. Emini.** 1995. Turnover of circulating virion RNA and of cell-associated viral DNA reflects active viral replication in human immunodeficiency virus type 1-infected individuals. J. Virol. **69:**2637–2639.

44. **Liu, S.-L., T. Schacker, L. Musey, D. Shriner, M. J. McElrath, L. Corey, and J. I. Mullins.** 1997. Divergent pattern of progression to AIDS after infection from the same source: human immunodeficiency virus type 1 evolution and antiviral responses. J. Virol. **71:**4284–4295.

45. **Lukashov, V. V., C. L. Kuiken, and J. Goudsmit.** 1995. Intrahost human immunodeficiency virus type 1 evolution is related to length of the immunocompetent period. J. Virol. **69:**6911–6916.

46. **Mansky, L. M., and H. M. Temin.** 1995. Lower in vivo mutation rate of human immunodeficiency virus type 1 than that predicted from the fidelity of purified reverse transcriptase. J. Virol. **69:**5087–5094.

47. **Martin-Rico, P., C. Pedersen, P. Skinhoj, C. Nielsen, and B. O. Lindhardt.** 1995. Rapid development of AIDS in an HIV-1-antibody-negative homosexual man. AIDS **9:**95–96.

48. **McKeating, J. A., J. Gow, J. Goudsmit, L. H. Pearl, C. Mulder, and R. A. Weiss.** 1989. Characterization of HIV-1 neutralization escape mutants. AIDS **3:**777–784.

49. **McNearney, T., Z. Hornickova, R. Markham, A. Birdwell, M. Arens, A. Saah, and L. Ratner.** 1992. Relationship of human immunodeficiency virus type 1 sequence heterogeneity to stage of disease. Proc. Natl. Acad. Sci. USA **89:**10247–10251.

50. **McRae, B., J. A. Lange, M. S. Ascher, F. de Wolf, H. W. Sheppard, J. Goudsmit, and J. P. Allain.** 1991. Immune response to HIV p24 core protein during the early phases of human immunodeficiency virus infection. AIDS Res. Hum. Retroviruses **7:**637–643.

51. **Mellors, J. W., L. A. Kingsley, C. Rinaldo, Jr., J. A. Todd, B. S. Hoo, R. P. Kokka, and P. Gupta.** 1995. Quantitation of HIV-1 RNA in plasma predicts outcome after seroconversion. Ann. Intern. Med. **122:**573–579.

52. **Mellors, J. W., C. R. J. Rinaldo, P. Gupta, R. M. White, J. A. Todd, and L. A. Kingsley.** 1996. Prognosis in HIV-1 infection predicted by the quantity of virus in plasma. Science **272:**1167–1170.

53. **Meyerhans, A., R. Cheynier, J. Albert, M. Seth, S. Kwok, J. Sninsky, L. Morfeldt-Månson, B. Asjö, and S. Wain-Hobson.** 1989. Temporal fluctuations in HIV quasispecies in vivo are not reflected by sequential HIV isolations. Cell **58:**901–910.

54. **Montefiori, D. C., G. Pantaleo, L. M. Fink, J. T. Zhou, J. Y. Zhou, M. Bilska, G. D. Miralles, and A. S. Fauci.** 1996. Neutralizing and infection-enhancing antibody responses to human immunodeficiency virus type 1 in long-term nonprogressors. J. Infect. Dis. **173:**60–67.

55. **Mulder, J., N. McKinney, C. Christopherson, J. Sninsky, L. Greenfield, and S. Kwok.** 1994. Rapid and simple PCR assay for quantitation of human immunodeficiency virus type 1 RNA in plasma: application to acute retro-

viral infection. J. Clin. Microbiol. **32:**292–300.

56. **Mullins, J. I.** 1988. Molecular aspects of the FeLV and SIV AIDS models, p. 43–49. *In* M. Girard and L. Valette (ed.), Retroviruses of human AIDS and related animal diseases. Pasteur Vaccins, Paris, France.

57. **Nowak, M. A., R. M. Anderson, A. R. McLean, T. F. Wolfs, J. Goudsmit, and R. M. May.** 1991. Antigenic diversity thresholds and the development of AIDS. Science **254:**963–969.

58. **Nowak, M. A., and A. J. McMichael.** 1995. How HIV defeats the immune system. Sci. Am. **1995**(8):58–65.

59. **Oka, S., S. Ida, T. Shioda, Y. Takebe, N. Kobayashi, K. Shibuya, K. Ohyama, K. Momota, S. Kimura, and K. Shimada.** 1994. Genetic analysis of HIV-1 during rapid progression to AIDS in an apparently healthy man. AIDS Res. Hum. Retroviruses **10:**271–277.

60. **Overbaugh, J., L. M. Rudensey, M. D. Papenhausen, R. E. Benveniste, and W. R. Morton.** 1991. Variation in simian immunodeficiency virus *env* is confined to V1 and V4 during progression to simian AIDS. J. Virol. **65:** 7025–7031.

61. **Pang, S., Y. Shlesinger, E. S. Daar, T. Moudgil, D. D. Ho, and I. S. Y. Chen.** 1992. Rapid generation of sequence variation during primary HIV-1 infection. AIDS **6:**453–460.

62. **Pantaleo, G., S. Menzo, M. Vaccarezza, C. Graziosi, O. J. Cohen, J. F. Demarest, D. Montefiori, J. M. Orenstein, C. Fox, L. K. Schrager, et al.** 1995. Studies in subjects with long-term nonprogressive human immunodeficiency virus infection. N. Engl. J. Med. **332:**209–216.

63. **Pathak, V. K., and H. M. Temin.** 1990. Broad spectrum of in vivo forward mutations, hypermutations, and mutational hotspots in a retroviral shuttle vector after a single replication cycle: substitutions, frameshifts, and hypermutations. Proc. Natl. Acad. Sci. USA **87:**6019–6023.

64. **Phillips, A. N., C. A. Lee, J. Elford, G. Janossy, A. Timms, M. Bofill, and P. B. A. Kernoff.** 1991. Serial CD4 lymphocyte counts and the development of AIDS. Lancet **337:**389–392.

65. **Phillips, R. E., S. Rowland-Jones, D. F. Nixon, F. M. Gotch, J. P. Edwards, A. O. Ogunlesi, J. G. Elvin, J. A. Rothbard, C. R. M. Bangham, C. R. Rizza, and A. J. McMichael.** 1991. Human immunodeficiency virus genetic variation that can escape cytotoxic T cell recognition. Nature **354:**453–459.

66. **Piatak, M., M. S. Saag, L. C. Yang, S. J. Clark, J. C. Kappes, K.-C. Luk, B. H. Hahn, G. M. Shaw, and J. D. Lifson.** 1993. High levels of HIV-1 in plasma during all stages of infection determined by competitive PCR. Science **259:**1749–1754.

67. **Richman, D. D., D. Havlir, J. Corbeil, D. Looney, C. Ignacio, S. A. Spector, J. Sullivan, S. Cheeseman, K. Barringer, D. Pauletti, C.-K. Shih, M. Myers, and J. Griffin.** 1994. Nevirapine resistance mutations of human immunodeficiency virus type 1 selected during therapy. J. Virol. **68:**1660–1666.

68. **Rinaldo, C., X.-L. Huang, Z. Fan, M. Ding, L. Beltz, A. Logar, D. Panicali, G. Mazzara, J. Liebmann, M. Cottrill, and P. Gupta.** 1995. High levels of anti-human immunodeficiency virus type 1 (HIV-1) memory cytotoxic T-lymphocyte activity and low viral load are associated with lack of disease in HIV-1-infected long-term nonprogressors. J. Virol. **69:**5838–5842.

69. **Riviere, Y., M. B. McChesney, F. Porrot, F. Tanneau-Salvadori, P. Sansonetti, O. Lopez, G. Pialoux, V. Feuillie, M. Mollereau, S. Chamaret, et al.** 1995. Gag-specific cytotoxic responses to HIV type 1 are associated with a decreased risk of progression to AIDS-related complex or AIDS. AIDS Res. Hum. Retroviruses **11:**903–907.

70. **Roberts, J. D., K. Bebenek, and T. A. Kunkel.** 1988. The accuracy of reverse transcriptase from HIV-1. Science **242:**1171–1173.

71. **Saitou, N., and M. Nei.** 1987. The neighbor-joining method: a new method for reconstructing phylogenetic trees. Mol. Biol. Evol. **4:**406–425.

72. **Schmidt, G., K. Amiraian, H. Frey, J. Wethers, R. W. Stevens, and D. S. Berns.** 1989. Monitoring human immunodeficiency virus type 1-infected patients by ratio of antibodies to gp41 and p24. J. Clin. Microbiol. **27:**843–848.

73. **Shannon, C. E., and W. Weaver.** 1949. The mathematical theory of communication. University of Illinois Press, Urbana, Ill.

74. **Sheppard, H. W., M. S. Ascher, B. McRae, R. E. Anderson, W. Lang, and J. Allain.** 1991. The initial immune response to HIV and immune system activation determine the outcome of HIV disease. J. Acquired Immune Defic. Syndr. **4:**704–712.

75. **Sheppard, H. W., W. Lang, M. S. Ascher, E. Vittinghoff, and W. Winkelstein.** 1993. The characterization of non-progressors: long term HIV-1 infection

with stable CD4+ T-cell levels. AIDS **7:**1159–1166.

76. **Simmonds, P., P. Balfe, C. A. Ludlam, J. O. Bishop, and A. J. Leigh Brown.** 1990. Analysis of sequence diversity in hypervariable regions of the external glycoprotein of human immunodeficiency virus type 1. J. Virol. **64:**5840–5850.

77. **Simmonds, P., P. Balfe, J. F. Peutherer, C. A. Ludlam, J. O. Bishop, and A. J. Leigh Brown.** 1990. Human immunodeficiency virus-infected individuals contain provirus in small numbers of peripheral mononuclear cells and at low copy numbers. J. Virol. **64:**864–872.

78. **Simmonds, P., L. Q. Zhang, F. McOmish, P. Balfe, C. A. Ludlam, and A. J. Leigh Brown.** 1991. Discontinuous sequence change of human immunodeficiency virus (HIV) type 1 *env* sequences in plasma viral and lymphocyte-associated proviral populations in vivo: implications for models of HIV pathogenesis. J. Virol. **65:**6266–6276.

79. **Sinicco, A., R. Fora, M. Sciandra, A. Lucchini, P. Caramello, and P. Gioannini.** 1993. Risk of developing AIDS after primary acute HIV-1 infection. J. Acquired Immune Defic. Syndr. **6:**575–581.

80. **Strathdee, S. A., J. W. Frank, J. McLaughlin, M. Leblanc, C. Major, M. V. O'Shaughnessy, and S. E. Read.** 1995. Quantitative measures of human immunodeficiency virus-specific antibodies predict progression to AIDS. J. Infect. Dis. **172:**1375–1379.

81. **Tersmette, M., R. A. Gruters, F. de Wolf, R. E. Y. de Goede, J. M. A. Lange, P. T. A. Schellekens, J. Goudsmit, H. G. Huisman, and F. Miedema.** 1989. Evidence for a role of virulent human immunodeficiency virus (HIV) variants in the pathogenesis of acquired immunodeficiency syndrome: studies on sequential HIV isolates. J. Virol. **63:**2118–2125.

82. **Thompson, J. D., D. G. Higgins, and T. J. Gibson.** 1994. CLUSTAL W: improving the sensitivity of progressive multiple sequence alignment through sequence weighting, position-specific gap penalties and weight matrix choice. Nucleic Acids Res. **22:**4673–4680.

83. **Wain-Hobson, S.** 1993. Viral burden in AIDS. Nature **366:**22.

84. **Wei, X., S. K. Ghosh, M. E. Taylor, V. A. Johnson, E. A. Emini, P. Deutsch, J. D. Lifson, S. Bonhoeffer, M. A. Novak, B. H. Hahn, M. S. Saag, and G. M. Shaw.** 1995. Viral dynamics in human immunodeficiency virus type 1 infection. Nature **373:**117–126.

85. **Weiss, R.** 1996. HIV receptors and the pathogenesis of AIDS. Science **272:**1885–1886.

86. **Wolfs, T. F., J. J. de Jong, H. Van den Berg, J. M. Tijnagel, W. J. Krone, and J. Goudsmit.** 1990. Evolution of sequences encoding the principal neutralization epitope of human immunodeficiency virus 1 is host dependent, rapid, and continuous. Proc. Natl. Acad. Sci. USA **87:**9938–9942.

87. **Wolfs, T. F., G. Zwart, M. Bakker, and J. Goudsmit.** 1992. HIV-1 genomic RNA diversification following sexual and parenteral virus transmission. Virology **189:**103–110.

88. **Wolfs, T. F., G. Zwart, M. Bakker, M. Valk, C. L. Kuiken, and J. Goudsmit.** 1991. Naturally occurring mutations within HIV-1 V3 genomic RNA lead to antigenic variation dependent on a single amino acid substitution. Virology **185:**195–205.

89. **Wolinsky, S. M., B. T. M. Korber, A. U. Neumann, M. Daniels, K. J. Kunstman, A. J. Whetsell, M. R. Furtado, Y. Cao, D. D. Ho, J. T. Safrit, and R. A. Koup.** 1996. Adaptive evolution of human immunodeficiency virus-type 1 during the natural course of infection. Science **272:**537–542.

90. **Zhang, L. Q., P. MacKenzie, A. Cleland, E. C. Holmes, A. J. Leigh Brown, and P. Simmonds.** 1993. Selection for specific sequences in the external envelope protein of human immunodeficiency virus type 1 upon primary infection. J. Virol. **67:**3345–3356.

91. **Zhang, Y.-M., S. C. Dawson, D. Landsman, H. C. Lane, and N. P. Salzman.** 1994. Persistence of four related human immunodeficiency virus subtypes during the course of zidovudine therapy: relationship between virion RNA and proviral DNA. J. Virol. **68:**425–432.

92. **Zhu, T., H. Mo, N. Wang, D. S. Nam, Y. Cao, R. A. Koup, and D. D. Ho.** 1993. Genotypic and phenotypic characterization of HIV-1 in patients with primary infection. Science **261:**1179–1181.

93. **Zwart, G., L. van der Hoek, M. Valk, M. T. Cornelissen, E. Baan, J. Dekker, M. Koot, C. L. Kuiken, and J. Goudsmit.** 1994. Antibody responses to HIV-1 envelope and gag epitopes in HIV-1 seroconverters with rapid versus slow disease progression. Virology **201:**285–293.